



Variable Sampling Intervals in Shewhart Charts Based on Stochastic Failure Time Modelling

Rainer Göb¹, Maria Fernanda Ramalhoto² and Antonio Pievatolo³

¹Institute for Applied Mathematics and Statistics, University
of Würzburg, Sanderring, Würzburg, Germany

²Instituto Superior Técnico, Mathematics Department,
Av. Rovisco Pais, Lisbon, Portugal

³CNR-IMATI, Via Bassini, Milano, Italy
(Received January 2005, accepted March 2006)

Abstract: Shewhart charts with variable sampling intervals (VSI) have received considerable interest in academic literature. For industrial practice, three aspects of VSI schemes are of vital interest: i) a simple algorithm for switching, i.e., varying sampling intervals, which can easily be executed on shop floor, ii) a simple design of the charts, and iii) flexible model assumptions on the time to failure in the process, which are able to express phenomena of tool wear, aging of equipment, wear out of adjustment devices etc. VSI schemes suggested by literature often tend to fall short in these respects. The present paper suggests a novel framework for VSI policies based on the distribution of the time to failure in the process, with a very simple and easily executable switching algorithm. The distribution of time to failure is assumed to be a member of the Weibull family, which is rich enough to model a large class of aging phenomena. The design parameters of VSI charts can be determined easily from graphs. It is shown that VSI charts considerably outperform fixed sampling interval charts with respect to the time of out-of-control operation.

Keywords: Bipartition policy, false alarms, inherent degradation, Shewhart control charts, variable sampling interval.

1. Introduction

The Shewhart control charting scheme, as exposed by textbooks and industrial standards, formally defines the way of evaluating samples, the relevant test statistics, e.g., \bar{X} or S , control limits, e.g., three-sigma limits, and the alarm rule. However, the *sampling distance* or *sampling interval*, i.e., the time interval between successive samples, is left to informal reasoning. Implicitly, textbooks assume *fixed sampling interval (FSI)* policies, i.e., time intervals of identical and constant length between successive samples. Only under an FSI policy the *average run length (ARL)* is a reasonable performance measure for control charts. FSI policies are simple in administration, and hence very popular in industrial practice. Nevertheless, sampling intervals are sometimes varied by practitioners on an ad hoc basis. Strategies of changing the sampling interval or the sampling distance are denoted as *variable sampling interval (VSI)* strategies. Three motivations for the use of VSI approaches can be identified.

- (i) Observation of suspect samples where the test statistic is close to the control limits without violating them, e.g., beyond 1 sigma limits or beyond 2 sigma limits. Such samples may indicate an out-of-control operation of the process. Hence it seems reasonable to increase the sampling frequency afterwards.

- (ii) Occurrence of corrective interventions onto the process, like adjustments or repairs. Afterwards, the sampling frequency is increased to check whether the intervention had the desired effect on process operation.
- (iii) Knowledge of inherent laws of deterioration or aging of the process equipment or the process environment. With increasing operation time the process is increasingly prone to unwelcome substantial variation, i.e., inadequate operation, failure, or breakdown. Hence, with increasing operation time, the sampling frequency is successively increased so as to achieve early detection of out-of-control operation.

Motivation (i) has received considerable interest in literature. Shewhart charts based on (i) were investigated by [12], [15], [14], [13], [17], [18], [1], [16], [4], [10], [9], for instance. It is difficult to reflect the motivation (ii) by a formal and general stochastic model. Essentially, motivation (ii) requires a phase I period of control charting, i.e., stable in-control operation is restored and the control chart is retuned. Hitherto, motivation (iii) has received little attention only. Ramalhoto *et al.* [11] outline a general model of monitoring aging processes based on (iii).

Ideas (i) and (iii) require some insight into the stochastic mechanism of substantial variation (failures, shifts) in the process, i.e., into the distribution of time to failure. Such knowledge is not considered by Shewhart's [20] original approach. However, the application fields of control charts have been changing and enlarging, see [19]. There may be cases where the failure time distribution is completely unknown, or where shifts from the in-control to the out-of-control state are completely unpredictable or chaotic, e.g., operators' fault. In modern manufacturing or service industry, plants, machines, staff, process history are continuously documented and analyzed for maintenance and improvement purposes. In many cases, there is sufficient information to establish stochastic models of tool wear, process degradation or aging. Throughout, VSI approaches based on the idea (i) stipulate exponentially distributed times between process failures. Studies based on the idea (iii) have to be based on more general and flexible classes of failure time distributions like Weibull distribution.

Two aspects are crucial for successful implementation of control charts on shop floor: *Simplicity* of the control algorithm and the chart design, and *generality* and *flexibility* of the underlying model assumptions. Simplicity and generality made the FSI Shewhart chart a success in industry. VSI approaches are more flexible. However, they tend to fall short in simplicity. In particular, approaches based on idea (i) may be difficult in administration due to frequent and unscheduled changes of the sampling distance. The organizational difficulties in implementing such VSI strategies are pointed out by Baxley [2].

The present paper elaborates upon idea (iii), i.e., VSI control charting policies motivated by knowledge on inherent degradation or aging of the process. We choose the Shewhart chart as the control chart paradigm to illustrate the VSI design approach, because of three properties of the Shewhart scheme: i) simple analytical manipulation, ii) straightforward understanding and interpretation, iii) by far of the highest popularity in industrial practice. To achieve the requested properties of simplicity, generality and flexibility of the VSI design, the following features of the control policy are important: 1) Changes in the sampling interval are fixed along the time axis in a predetermined schedule. 2) Changes in the sampling interval are infrequent. 3) Primary interest is not in deriving the policy parameters as optimum solutions under a specific model. Instead, it is shown that a simply designed VSI chart considerably outperforms a comparable FSI chart under a variety of failure time models expressed by Weibull distributions.

The paper is organized in the following way. Section 2 establishes a dynamic model of process quality and explains the control charting procedure. Section 3 defines VSI and FSI sampling policies in a formal manner. Section 4 provides formulae for the expected time of out-of-control operation and the expected number of false alarms. Section 5 suggests a simple design for VSI charts: the bipartition policy with one switching time, based on two rules labelled 1 and 2, and on experience gained on shop floor. Section 6 discusses the parameters of VSI charts under a scale family of failure time distribution. Graphs for determining VSI charts and for evaluating their performance are given by section 7. A numerical example is given in section 8. Section 9 presents a conclusion and some suggestions for further research. In order to make the paper easier to be read, mathematical derivations are provided in the appendices A, B, and C.

2. Process and Sampling Model

Samples of n items with corresponding univariate quality characteristics X_{t1}, \dots, X_{tn} are taken from a process at sampling time $t > 0$. Successive samples are independent. Each sample X_{t1}, \dots, X_{tn} is independent and identically distributed where the distribution of X_{t1}, \dots, X_{tn} is characterized by a value θ_t of the *process quality parameter* θ . In most situations the usual univariate process quality parameters are the process mean $\theta = \mu = E[X]$ and the process variance $\theta = \sigma^2 = V[X]$. Sometimes in some of these situations it is useful to monitor both the mean and the variance, i.e., to consider the bivariate process quality parameter $\theta = (\mu, \sigma^2)$, as we did in section 7 for the Shewhart case.

At time 0 the process is assumed to be in an in-control state which is characterized by the *in-control value* $\theta_t = \theta_{in}$ of the parameter. At a random time $D > 0$ a *disturbance* or shock shifts the process from the in-control state to an out-of control state, where $P(D > 0) = 1$. In terms of the process parameter this amounts to a shift from the in-control value $\theta_t = \theta_{in}$ holding for $t < D$ to the out-of control value $\theta_t = \theta_{out}$ holding for $t \geq D$. The disturbance results from failure in machinery or equipment or in the process environment, e.g., by operators or service staff. Hence D is called *failure time*. In view of such failure sources a self-repair of the process is excluded – without a corrective intervention, after the failure time occurs the process continues in the out-of-control state. Statistical inference from process documentation data, from technical parameters of the equipment, including equipment reliability and maintenance strategies, provide knowledge on the distribution function F of the failure time D .

A control chart of Shewhart type is used to test the process for the presence of a shift in the quality parameter. At sampling time t , a real-valued statistic $T_t = T(X_{t1}, \dots, X_{tn})$ is compared to control limits $LCL < UCL$. An *alarm or out-of-control signal* is triggered iff $T_t \leq LCL$, or $T_t \geq UCL$. After an alarm, the process is *inspected* so as to detect the actual state of the process. If the inspection confirms the in-control state of the process (false alarm), the process continues without further intervention. If the process is actually out-of-control, the process is subject to a *corrective intervention*, e.g., adjustment, repair, or installation of new equipment. The corrective intervention removes the causes of failure and renews the process. The renewed process restarts in the in-control state.

The stochastic properties of the control chart are essentially characterized by the *conditional alarm probabilities*: the probability of a false alarm, i.e., the probability

$$p_{in} = P_{\theta_{in}}(T_t \leq LCL \text{ or } T_t \geq UCL) = P(T_t \leq LCL \text{ or } T_t \geq UCL | D > t) \quad (1)$$

of an alarm under the condition that the process is in control at time t , and the probability

$$p_{\text{out}} = P_{\theta_{\text{out}}}(T_t \leq LCL \text{ or } T_t \geq UCL) = P(T_t \leq LCL \text{ or } T_t \geq UCL | D \leq t) \quad (2)$$

of an alarm under the condition that the process is out of control at time t .

3. Arrangement of Sampling Times

In a VSI policy, the sampling distances are changing along the time axis. We consider $s+1$ different sampling distances h_0, h_1, \dots, h_s . Let k_0, \dots, k_{s-1} be positive integers, let $k_s = +\infty$, and let the times a_l be defined by

$$a_0 = 0, \quad a_l = k_0 h_0 + \dots + k_{l-1} h_{l-1} \quad \text{for } l = 1, \dots, s \quad (3)$$

The sampling times $t_1 < t_2 < t_3 \dots$ are arranged as multiples of the sampling distances according to the following rule:

$$t_{k_0 + \dots + k_{l-1} + i} = \begin{cases} ih_0 & \text{for } i = 1, 2, \dots, k_0, l = 0, \\ a_l + ih_l & \text{for } i = 1, 2, \dots, k_l, l = 1, \dots, s, \end{cases} \quad (4)$$

i.e., the sampling distance is changed from h_{l-1} to h_l at the *switching time* a_l for $l = 1, \dots, s-1$, and remains stable at h_s after the last switching time a_s .

A proper VSI *policy or switching policy* is characterized by the sampling distances h_0, \dots, h_s with $h_l \neq h_{l-1}$, the interval numbers k_0, k_1, \dots, k_s , and the switching rules expressed by equations (3) and (4). A FSI policy can be considered as an instance of the same scheme with identical sampling distances $h = h_l$.

If sampling distances become too small the assumption of independent samples made in section 2 may be violated. This is a general objection against VSI policies. However, the VSI policy considered in section 5, below, prescribes few switches so that the smallest sampling distance achieved is still large enough to maintain the independence assumption. See also the numerical example in section 8. The discussion of autocorrelated process data is out of the scope of the paper and should be considered separately, see the discussion in the conclusion, section 9.

4. The Renewal Cycle and its Characteristics

A *renewal cycle* is the period between the start of the process at a time 0 and the first alarm in the out-of-control state of the process. After this alarm, the out-of-control state is detected. The process is *renewed*, i.e., the effect of the disturbance is removed and the process is restarted in the in-control state. Under this assumption, the stochastic characteristics of successive cycles, like cycle length, number of false alarms, time of disturbance, are independent and identically distributed and constitute a simple *renewal process*. In this simple situation we can omit a time index in the cycle characteristics.

We consider the following stochastic cycle characteristics:

- The *cycle length* Z , i.e. the time of the first alarm in the out-of-control state.
- The time $O = Z - D$ of out-of-control operation.
- The number A_{false} of false alarms, i.e. the number of sampling times $t_i < D$ before the disturbance time D , where an alarm is signalled.

We are interested in the expectations of these cycle characteristics. The *average cycle length*,

i.e., the expectation $\mu_Z = E[Z]$ of the cycle length, is calculated in appendix B:

$$\mu_Z = E[Z] = \sum_{m=0}^s \sum_{i=0}^{k_m-1} \Delta_{m,i} \bar{F}(a_m + ih_m), \tag{5}$$

where for $m=0, \dots, s$, $i=0, \dots, k_m-1$, we let

$$\Delta_{m,i} = \begin{cases} \frac{h_0}{p_{out}} + \sum_{l=1}^s (h_l - h_{l-1}) \frac{(1 - p_{out})^{k_0 + \dots + k_{l-1}}}{p_{out}}, & \text{if } m=0=i \\ h_m + \sum_{l=1}^{s-m} (h_{m+l} - h_{m+l-1}) (1 - p_{out})^{k_m + \dots + k_{m+l-1} - i}, & \text{otherwise} \end{cases}, \tag{6}$$

and where $\bar{F} = 1 - F$ is the complement of the cumulative distribution function of the disturbance time (failure time) D . The average time of out-of-control operation is given by

$$\mu_O = E[O] = E[Z] - E[D] = \mu_Z - \mu_D. \tag{7}$$

The *average number of false alarms*, i.e., the expectation $\mu_{A_{false}} = E[A_{false}]$ of the number of false alarms, is calculated in appendix C:

$$\mu_{A_{false}} = E[A_{false}] = p_{in} \sum_{m=0}^s \sum_{i=0}^{k_m-1} \bar{F}(a_m + ih_m). \tag{8}$$

5. A Simple Design for VSI Charts

The design of control charts has received enormous interest. In particular, starting with Duncan's [5] pioneering work, various authors have suggested economically optimum designs based on economic loss functions. See [8], [3] or [6] for literature surveys. However, economic designs have not gained popularity in industry, essentially because of their complexity. In particular, the following issues are important: 1) it is difficult and time consuming to determine economic parameters, e.g., because of missing or inaccessible cost allocations, 2) adaptation to changes in the economic environment can be intolerably slow, 3) the numerical computation of economically optimum designs is involved and is not supported by statistical packages, and 4) restrictions and costs of administration on shop floor are not taken into account by economically optimum design schemes.

In industry, the design parameters of control charts are often chosen arbitrarily or possibly by experience. Sample sizes usually range from $n=1$ to $n=10$, with $n=3, 5, 7$ as customary choices. Three-sigma limits are the preferred choice for control limits. The most important criteria for determining the sampling distance are frequently related to shop floor administration and insights regarding process failures. It is often recommended to sample more frequently as a tool or machine approaches the end of its cycle in order to prevent against poor quality. Typically, Wheeler ([21], p. 142) states that "it is the rate at which the process can change that determines the rationality of the sampling frequency". From a formal point of view this amounts to studying the distribution F of the time D to failure in the process, an approach which is addressed by the present paper.

In the sequel, we distinguish between the VSI *policy* and the *design* of a specific VSI chart. The VSI switching policy provides a general rule for changing the sampling distances and for determining the number of switching times. In the framework of a VSI policy, the design of a VSI chart consists of sample size, control limits, and a specific choice of sampling distances and switching times.

Let us first consider the design of a specific VSI chart in the framework of a given VSI switching policy. We do not establish an objective function to derive optimum charts. Instead, we use a *comparative design* approach. In a given practical context, we assume that a FSI chart with sample size n , control limits LCL and UCL , sampling distance h is designed using some rational considerations. In the comparative design, the sample size n and the control limits LCL , UCL shall be the same for the FSI and for the VSI chart. For the FSI chart with sampling distance h and for the VSI chart with switching parameters h_0, \dots, h_s , k_0, \dots, k_{s-1} , consider the average times

$$\mu_O(h), \mu_O(h_0, \dots, h_s, k_0, \dots, k_{s-1}) \quad (9)$$

of out-of-control operation and the average number

$$\mu_{A_{\text{false}}}(h), \mu_{A_{\text{false}}}(h_0, \dots, h_s, k_0, \dots, k_{s-1}) \quad (10)$$

of false alarms as functions of the parameters h and h_0, \dots, h_s , k_0, \dots, k_{s-1} , respectively. The comparative design proceeds by the following rule 1.

Rule 1 (Comparative design of a VSI chart from an FSI chart). *Let the sample size n and the control limits LCL , UCL be adopted from a given FSI chart with sampling distance h , and let a switching policy be prescribed. A VSI chart with parameters*

$$h_0 = h_0(h), \dots, h_s = h_s(h), \quad k_0 = k_0(h), \dots, k_{s-1} = k_{s-1}(h) \quad (11)$$

is determined by the following requirements:

(R1) *The expected sampling cost is the same for the FSI and the VSI chart, i.e.,*

$$\mu_{A_{\text{false}}}(h_0, \dots, h_s, k_0, \dots, k_{s-1}) = \mu_{A_{\text{false}}}(h). \quad (12)$$

(R2) *The expected time of out-of-control operation is minimum among all VSI charts conforming to the prescribed switching policy and satisfying equation (12).*

From the point of view of sampling cost the prescribed FSI chart and the VSI chart determined by rule 1 are equivalent. Hence among the two the chart with smaller expected out-of-control operation time is the one with better performance.

The comparative design by rule 1 can be applied to determine VSI charts under any VSI policy type. In view of current industrial practice it makes little sense to recommend VSI policies based on some optimality principle. Instead, we suggest a policy with the following properties: i) infrequent switching times, ii) simple scheduling of switching times according to the distribution of the time to failure in the process, and iii) easy integration into the administration of the production process. The policy is intended for the control of an *aging* process, i.e., with increasing operation time the process exhibits increasing proneness to failure. In this case it is reasonable to sample more often with increasing operation time, i.e., to reduce the sampling distance with increasing operation time. In the terminology of the switching model of section 3, this amounts to assume a decreasing sequence $h_0 > h_1 > \dots > h_s$ of sampling distances, as prescribed by the following *geometric degression policy* (rule 2).

Rule 2 (VSI degression switching policy). *In the geometric degression policy the sampling distances form a decreasing sequence $h_0 > h_1 > \dots > h_s$ structured by*

$$h_{i+1}/h_i = r \quad \text{for } i = 0, \dots, s-1 \quad (13)$$

with some degression parameter $0 < r < 1$. Two simple instances of the degression policy are:

- *Bipartition policy.* $r = h_{i+1}/h_i = 0.5$ for $i = 0, \dots, s-1$.
- *Bipartition policy with one switching time.* $s = 1$, $h_1/h_0 = 0.5$.

For industrial implementation, the bipartition policy with one switching time is preferable to make administration on the shop floor simple, and to make switching times infrequent. The subsequent section 7 investigates numerically the design by rule 1 under the simple bipartition policy with one switching time. It will be shown that the VSI chart outperforms the FSI chart for a large class of failure time distributions.

6. Scale Families of Failure Time Distribution

In a great variety of cases, the distribution function F of the time to failure is a member of a scale family (F_g) indexed by a positive scale parameter $g > 0$. The cumulative distribution functions in such a family are related by the equation

$$F_g(x) = F_1\left(\frac{x}{g}\right) \text{ for all } x, \text{ all } g > 0. \tag{14}$$

The two parameter Weibull distribution $WEI(g, \beta)$ is a member of the family of distributions indexed by the scale parameter g and the shape parameter β with cumulative distribution function

$$F_{g,\beta}(x) = \begin{cases} 0, & \text{if } x < 0, \\ 1 - \exp\left(-\left(\frac{x}{g}\right)^\beta\right), & \text{if } x \geq 0. \end{cases} \tag{15}$$

For an arbitrary scale family (F_g) , the influence of the scale parameter on the average cycle length and the average number of false alarms can be expressed by simple formulae. Consider the average time $\mu_O(h_0, \dots, h_s, k_0, \dots, k_{s-1}, g)$ of out-of-control operation and the average number $\mu_{A_{\text{false}}}(h_0, \dots, h_s, k_0, \dots, k_{s-1}, g)$ of false alarms as functions of the policy parameters $h_0, \dots, h_s, k_0, \dots, k_{s-1}$ and of the scale parameter g . Then obviously from formulae (3), (5), (6), (8), and (14)

$$\mu_O(h_0, \dots, h_s, k_0, \dots, k_{s-1}, g) = g \cdot \mu_O(h_0/g, \dots, h_s/g, k_0, \dots, k_{s-1}, 1), \tag{16}$$

$$\mu_{A_{\text{false}}}(h_0, \dots, h_s, k_0, \dots, k_{s-1}, g) = g \cdot \mu_{A_{\text{false}}}(h_0/g, \dots, h_s/g, k_0, \dots, k_{s-1}, 1), \tag{17}$$

Consider the comparative design by rule 1, i.e., let h be a prescribed FSI sampling distance and let the parameters $h_{i,g} = h_{i,g}(h)$, $k_{j,g} = k_{j,g}(h)$ of a corresponding VSI chart be determined by the requirements (R1) and (R2) of rule 1. From the requirements (R1) and (R2) and formulae (12), (16), (17), we obtain

$$h_{i,g}(h) = g h_{i,1}\left(\frac{h}{g}\right), \quad k_{j,g}(h) = k_{j,1}\left(\frac{h}{g}\right), \tag{18}$$

$$\begin{aligned} \mu_O(h_{0,g}(h), \dots, h_{s,g}(h), k_{0,g}(h), \dots, k_{s-1,g}(h), g) = \\ g \cdot \mu_O(h_{0,1}(h/g), \dots, h_{s,1}(h/g), k_{0,1}(h/g), \dots, k_{s-1,1}(h/g), 1) \end{aligned} \tag{19}$$

From formulae (18) and (19) it is clear that in investigating the comparative design of VSI charts by the rule 1 attention can be restricted to scale parameter $g = 1$.

7. The Performance of Bipartition Charts with One Switching Time

We compare the performance of FSI and VSI charts related one to each other by the design rule 1. The VSI policy is the simple bipartition type with one switching time described by rule 2. In this case, the VSI chart is characterized by the parameters h_0 , $h_1 = h_0/2$, k_0 , where h_0 is the sampling distance before switching, h_1 the sampling distance after switching, and where the integer k_0 is the number of samples taken before switching.

The comparison refers to the Shewhart chart due to its simplicity in analytics and interpretation, and because it remains the most popular in industrial practice. The controlled parameters are the process mean μ and the process variance σ^2 , i.e., we have $\theta = (\mu, \sigma^2)$ in the model of section 2. We consider two charts:

Chart 1: Two-sided Shewhart \bar{X} chart. The sample statistic at sampling time t is the sample average $\bar{X}_t = 1/n \sum_l X_{tl}$. The control limits are the three-sigma limits

$$LCL_{\bar{X}} = \mu_{in} - 3\sigma/\sqrt{n}, \quad UCL_{\bar{X}} = \mu_{in} + 3\sigma/\sqrt{n}, \quad (20)$$

the center line is fixed at μ_{in} . For the design of the chart, the in-control process variance is assumed to be known.

Chart 2: One-sided upper Shewhart S^2 chart. The sample statistic at sampling time t is the sample variance $S_t^2 = \frac{1}{n-1} \sum_l (X_{tl} - \bar{X}_t)^2$. The upper control limit is the three-sigma limit

$$UCL_{S^2} = \sigma_{in}^2 \left(1 + 3\sqrt{\frac{2}{n-1}} \right). \quad (21)$$

For the design of the chart, the in-control process variance is assumed to be known.

The S^2 chart is considered only in the combination $\bar{X}-S^2$ chart. The \bar{X} chart and the combined $\bar{X}-S^2$ charts are investigated under three shift models:

- (SM1) Shift in the process mean at time D of ρ units of process standard deviation, constant process variance; i.e., $\mu_t = \mu_{in}$ for $t < D$, $\mu_t = \mu_{out} = \mu_{in} + \rho\sigma$ for $t \geq D$, $\sigma_t^2 = \sigma^2$.
- (SM2) Shift in the process variance at time D by a factor κ^2 , constant process mean; i.e., $\sigma_t^2 = \sigma_{in}^2$ for $t < D$, $\sigma_t^2 = \sigma_{out}^2 = \kappa^2 \sigma_{in}^2$ for $t \geq D$, $\mu_t = \mu_{in}$.
- (SM3) Shifts both in the process mean and variance at time D ; i.e., $\mu_t = \mu_{in}$, $\sigma_t^2 = \sigma_{in}^2$ for $t < D$, $\mu_t = \mu_{out} = \mu_{in} + \rho\sigma_{in}$, $\sigma_t^2 = \sigma_{out}^2 = \kappa^2 \sigma_{in}^2$ for $t \geq D$.

For the evaluation of the charts we assume independent normally distributed quality characteristics X_{tl} . Under this assumption the sample statistics \bar{X}_t and S_t^2 at sampling time t are independent. \bar{X}_t has normal distribution $N(\mu, \sigma^2/n)$, $(n-1)S_t^2/\sigma^2$ has χ^2 -distribution with degree of freedom $n-1$. The alarm probabilities for the in-control states and the out-of-control states under the shift models (SM1), (SM2), (SM3) are displayed by Tables 1 and 2.

For the failure time distribution we will use the two parameter Weibull model $WEI(\vartheta, \beta)$ described by equation (15). Though sparse in parametrization, this distribution is flexible and permits a good fit to phenomena of aging equipment with failure rate

increasing over time. The estimation of the parameters of the Weibull model has been discussed extensively in literature (see [7] for a survey).

Table 1. Alarm probabilities for the \bar{X} chart under independent normally distributed quality characteristics, where Φ is the distribution function of standard normal distribution $N(0, 1)$.

Shift model	Alarm probability
In control	$p_{in} = 2 - 2\Phi(3)$
Out of control (SM 1)	$p_{out} = 1 - (\Phi(3 - \rho\sqrt{n}) - \Phi(-3 - \rho\sqrt{n}))$
Out of control (SM 2)	$p_{in} = 2 - 2\Phi\left(\frac{3}{k}\right)$
Out of control (SM 3)	$p_{out} = 1 - \left(\Phi\left(\frac{3 - \rho\sqrt{n}}{k}\right) - \Phi\left(\frac{-3 - \rho\sqrt{n}}{k}\right)\right)$

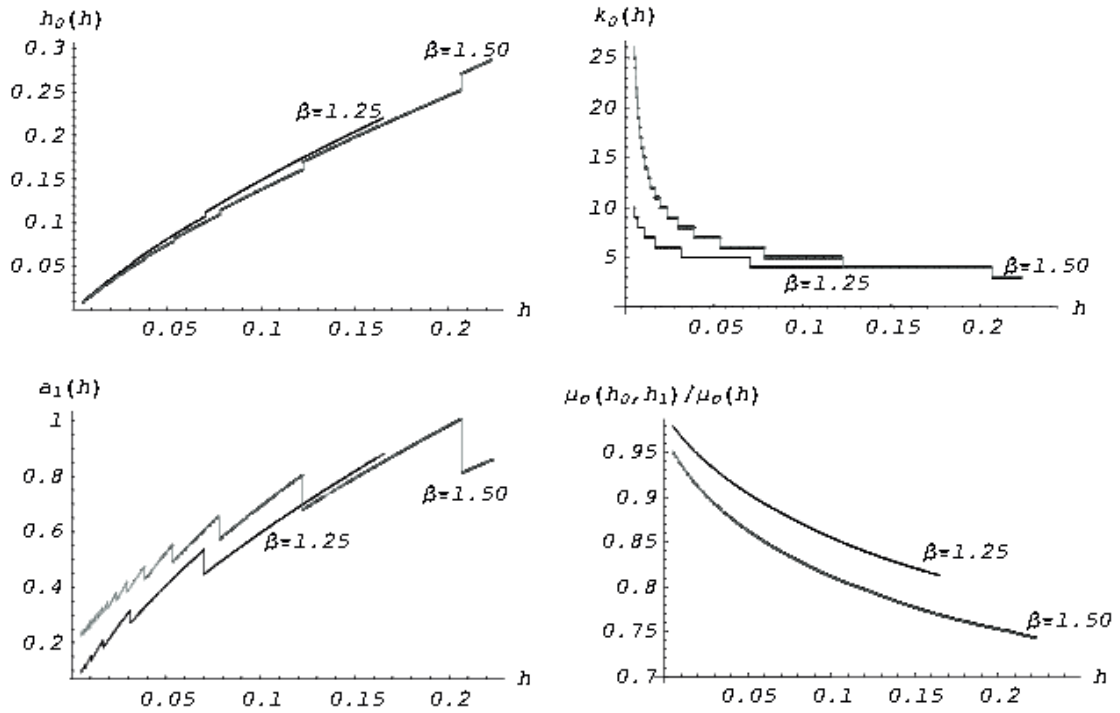
Table 2. Alarm probabilities for the $\bar{X} - S^2$ chart under independent normally distributed quality characteristics, where Φ is the distribution function of standard normal distribution $N(0, 1)$. F_{χ^2} is the distribution of χ^2 distribution with degree of freedom $n - 1$.

Shift model	Alarm probability
In control	$p_{in} = 1 - F_{\chi^2} \left(\left(1 + 3\sqrt{\frac{2}{n-1}}\right)(n-1) \right) (2\Phi(3) - 1)$
Out of control (SM 1)	$p_{out} = 1 - F_{\chi^2} \left(\left(1 + 3\sqrt{\frac{2}{n-1}}\right)(n-1) \right) (\Phi(3 - \rho\sqrt{n}) - \Phi(-3 - \rho\sqrt{n}))$
Out of control (SM 2)	$p_{out} = 1 - F_{\chi^2} \left(\left(1 + 3\sqrt{\frac{2}{n-1}}\right) \frac{n-1}{k^2} \right) (2\Phi\left(\frac{3}{k}\right) - 1)$
Out of control (SM 3)	$p_{out} = 1 - F_{\chi^2} \left(\left(1 + 3\sqrt{\frac{2}{n-1}}\right) \frac{n-1}{k^2} \right) (\Phi\left(\frac{3 - \rho\sqrt{n}}{k}\right) - \Phi\left(\frac{-3 - \rho\sqrt{n}}{k}\right))$

The two parameter Weibull distributions $WEI(\vartheta, \beta)$ constitute a scale family in ϑ (see section 6). Hence for the investigation of the performance of the VSI bipartition charts attention can be restricted to scale parameter $\vartheta = 1$.

As functions of a given FSI sampling distance h , figures 1 through 6 display the parameters of the corresponding VSI chart designed according to rule 2. For the sample size we consider the popular value $n = 5$. The results for $n = 3, 7, 9$ are similar and are displayed on the website <http://statistik.mathematik.uni-wuerzburg.de/projekte/shewart> charts. As well-known, the Weibull form parameter in an aging process satisfies $\beta > 1$ where $\beta = 1$ characterizes the memoryless exponential distribution. Hence values of β close to 1 are not relevant. For exemplifying the properties of the VSI chart, we consider the β values 1.25 (modest aging of the process), 1.50, 1.75, 2.25 (distinct aging of the process). In the framework of the three shift models (SM1), (SM2), (SM3) described on page 9 we consider moderate shifts only. Large parameter shifts are detected very quickly and are less interesting for comparing FSI and VSI policies. We consider a shift in the mean of $\rho = 1$ unit of standard deviation, i.e., a shift from μ_{in} to $\mu_{out} = \mu_{in} + \sigma$. For the shift in the variance, we consider an increase to double standard deviation, i.e., a shift from σ_{in} to $\sigma_{out} = 2\sigma_{in}$.

Weibull form parameter $\beta = 1.25$ and $\beta = 1.50$.



Weibull form parameter $\beta = 1.75$ and $\beta = 2.25$

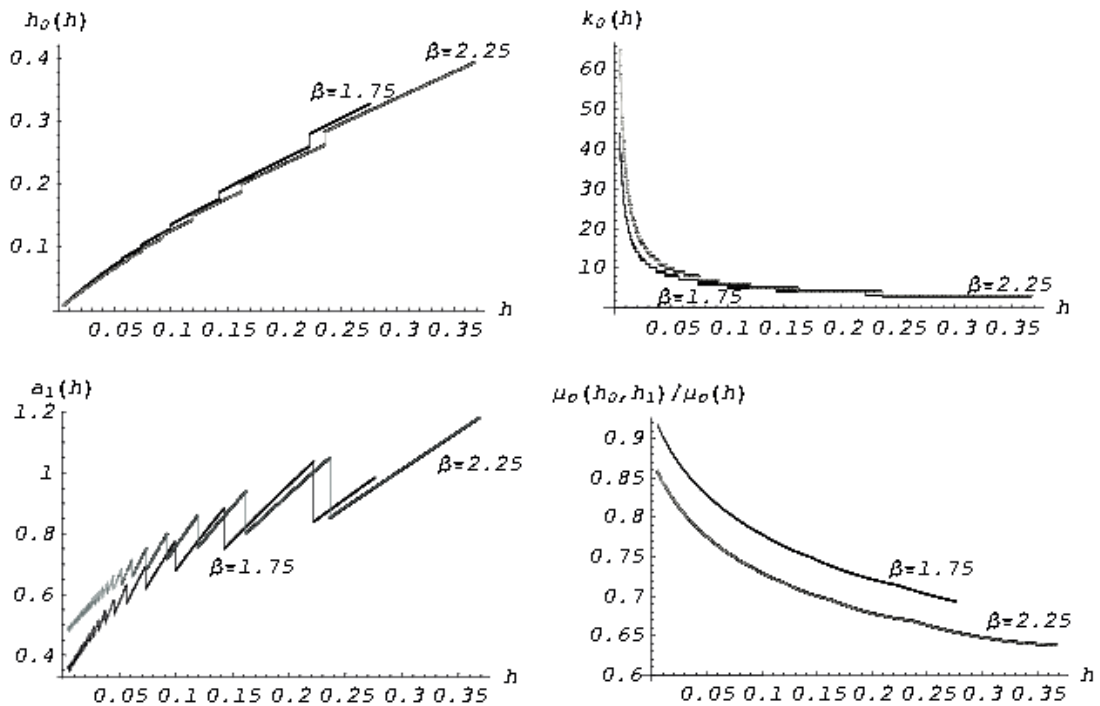
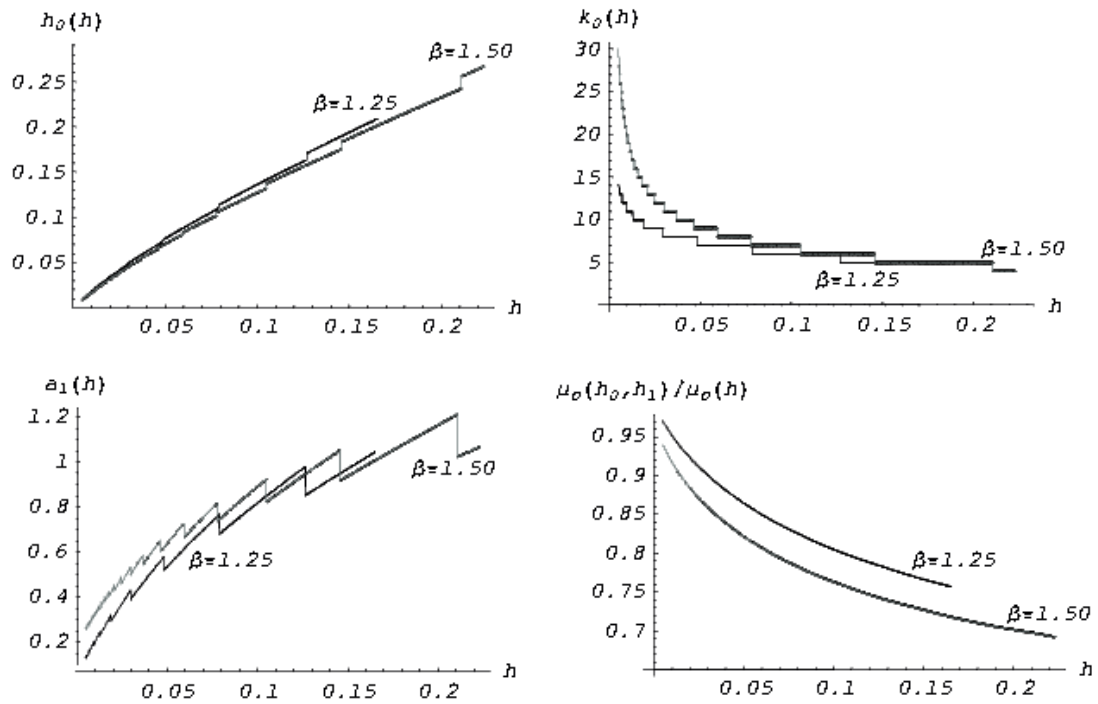


Figure 1. Comparison of FSI and VSI \bar{X} chart with sample size $n=5$ under out-of-control shift in the mean from μ_{in} to $\mu_{out} = \mu_{in} + \rho\sigma$, $\rho = 1.00$.

Weibull form parameter $\beta = 1.25$ and $\beta = 1.50$.



Weibull form parameter $\beta = 1.75$ and $\beta = 2.25$

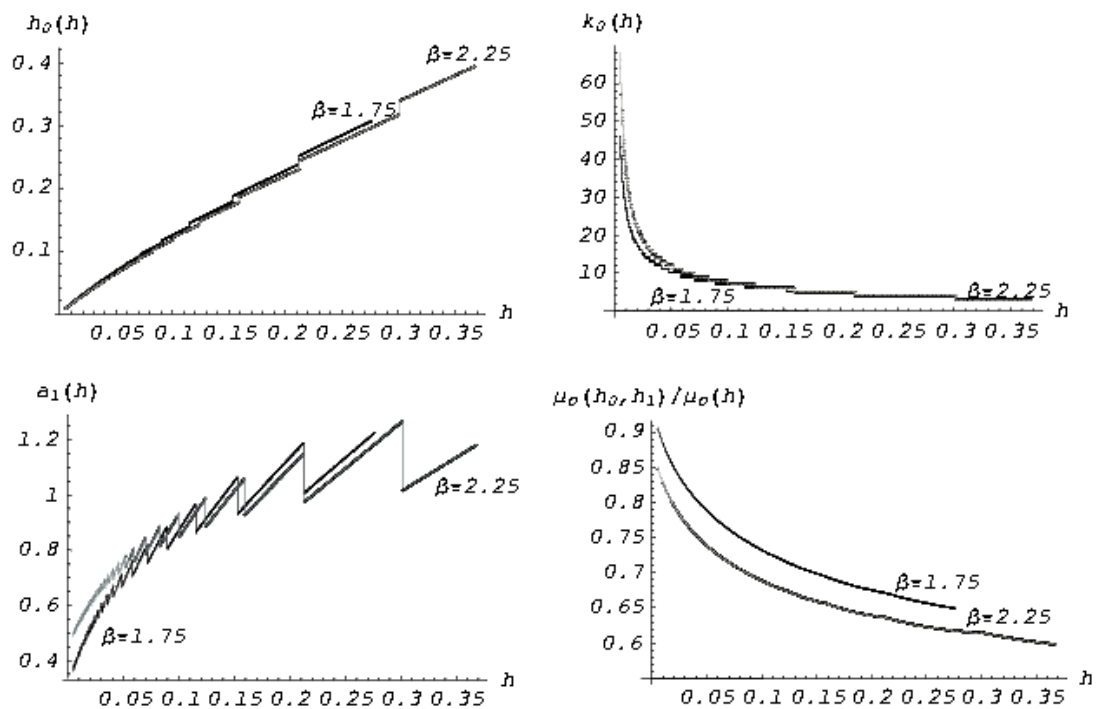
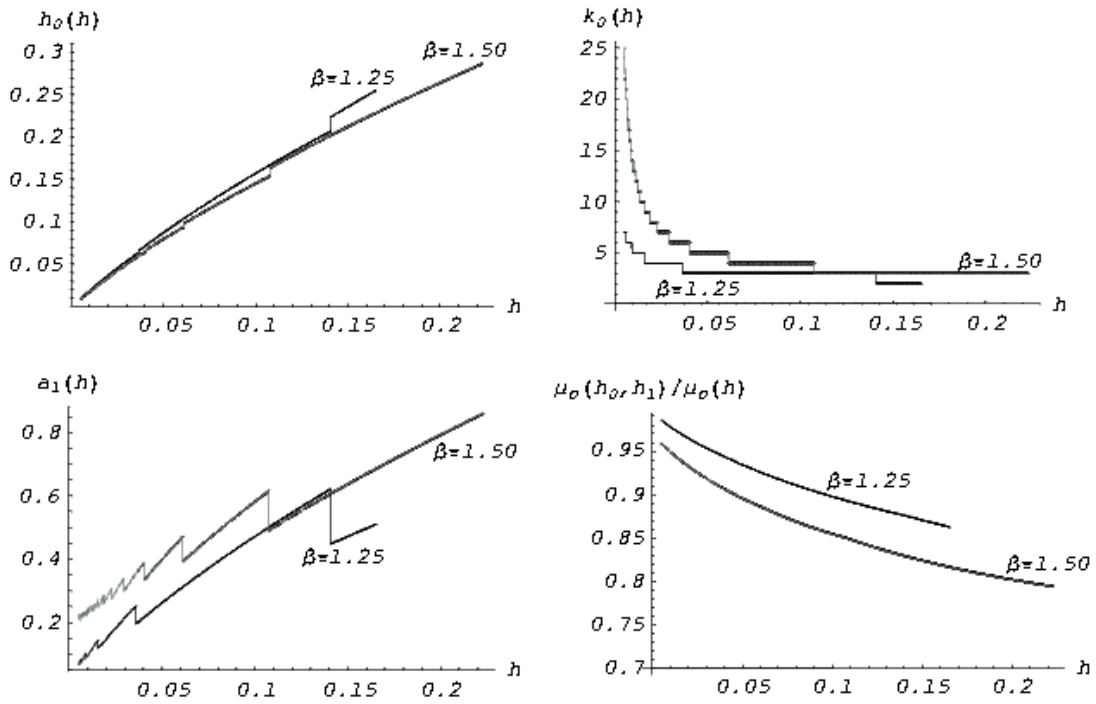


Figure 2. Comparison of FSI and VSI \bar{X} chart with sample size $n=5$ under out-of-control shift in the variance from σ_{in}^2 to $\sigma_{out}^2 = k^2 \sigma_{in}^2$, $k^2 = 2.00$.

Weibull form parameter $\beta = 1.25$ and $\beta = 1.50$.



Weibull form parameter $\beta = 1.75$ and $\beta = 2.25$

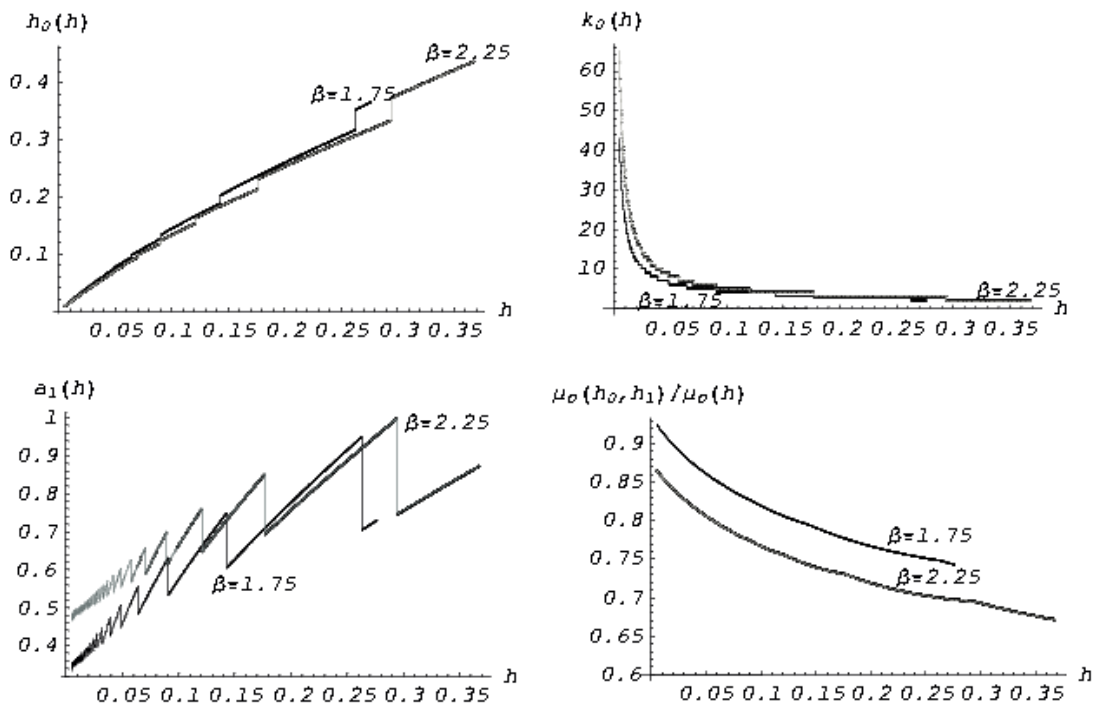
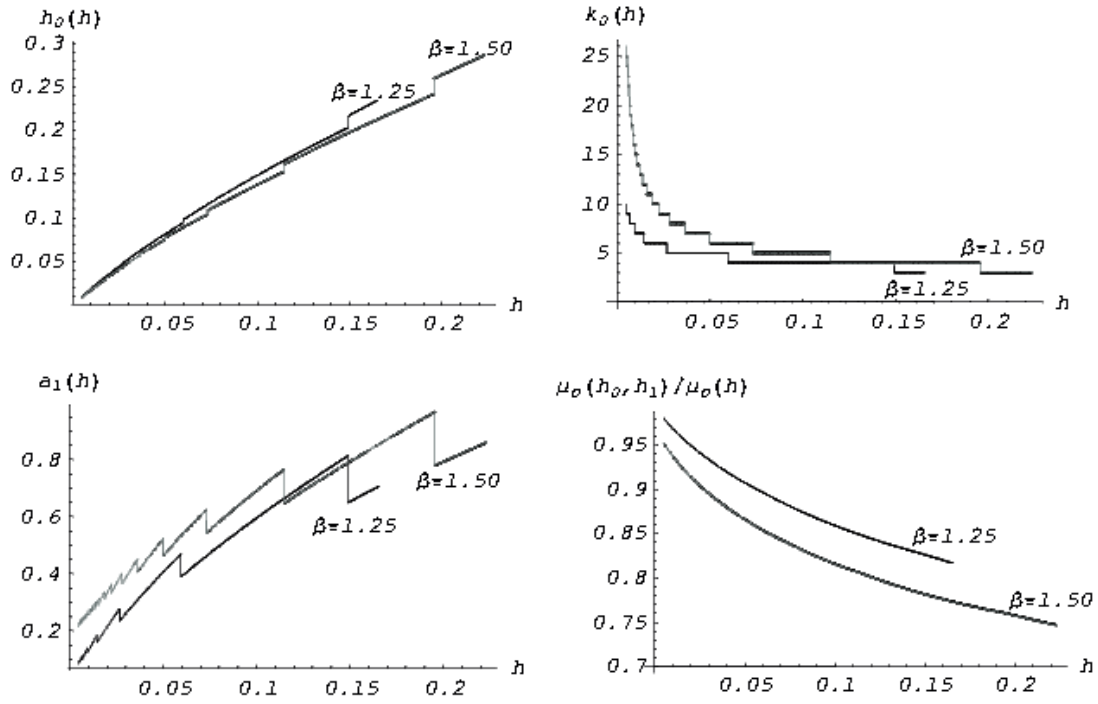


Figure 3. Comparison of FSI and VSI \bar{X} chart with sample size $n=5$ under out-of-control shift in the mean from μ_{in} to $\mu_{out} = \mu_{in} + \sigma_{in}$, and in the variance from σ_{in}^2 to $\sigma_{out}^2 = 2\sigma_{in}^2$.

Weibull form parameter $\beta = 1.25$ and $\beta = 1.50$.



Weibull form parameter $\beta = 1.75$ and $\beta = 2.25$

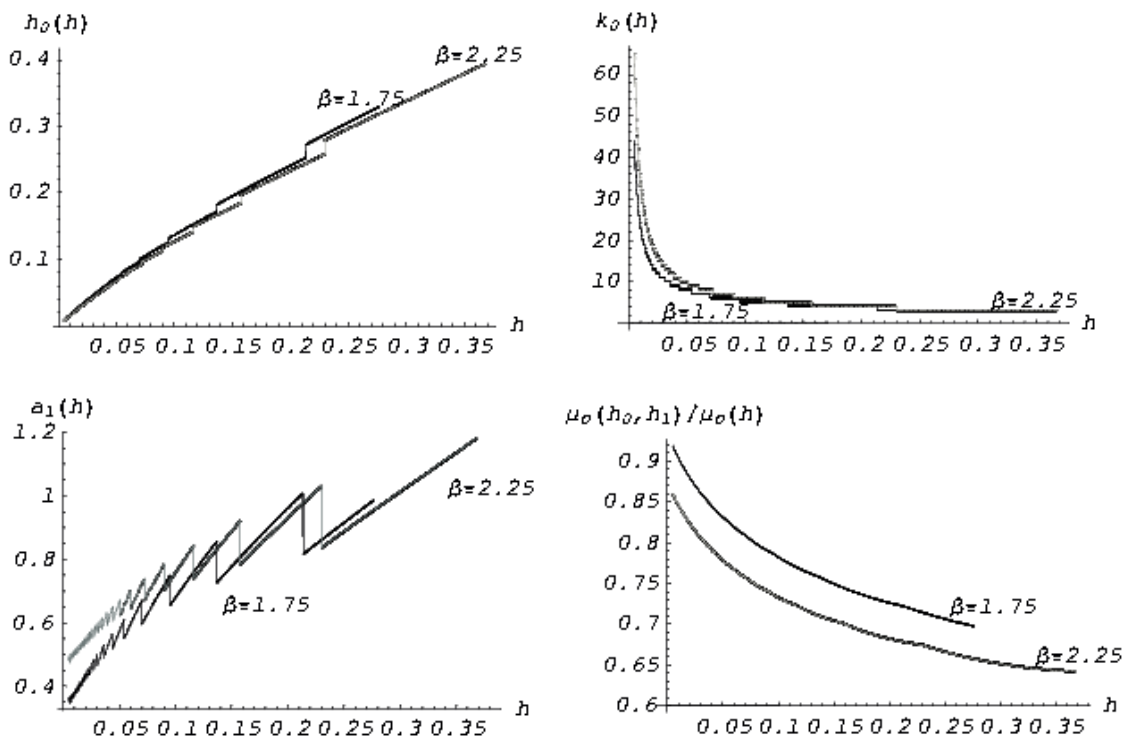
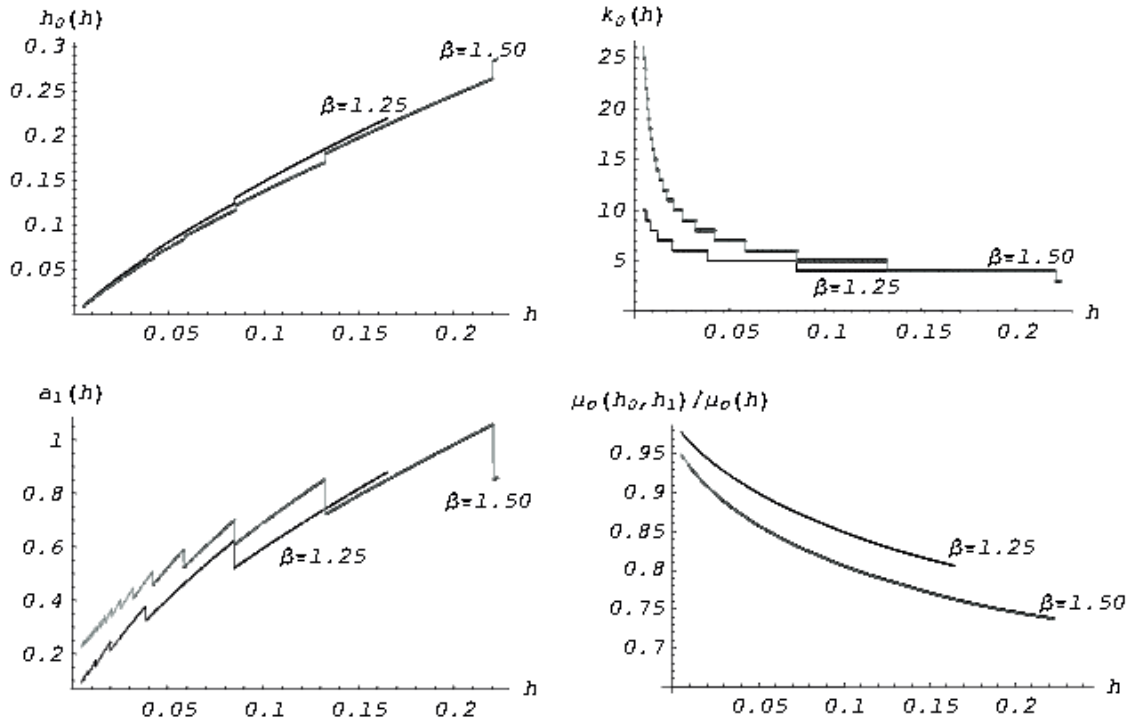


Figure 4. Comparison of FSI and VSI $\bar{X}-S^2$ chart with sample size $n=5$ under out-of-control shift in the mean from μ_{in} to $\mu_{out} = \mu_{in} + \rho\sigma$, $\rho = 1.00$.

Weibull form parameter $\beta = 1.25$ and $\beta = 1.50$.



Weibull form parameter $\beta = 1.75$ and $\beta = 2.25$

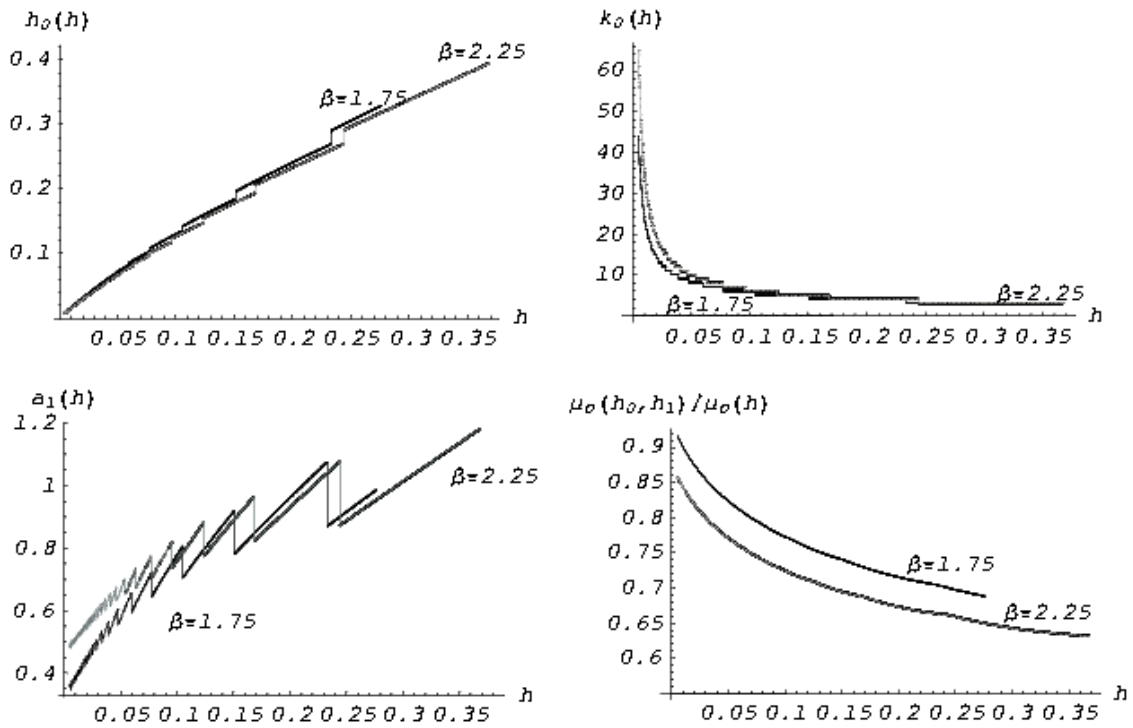
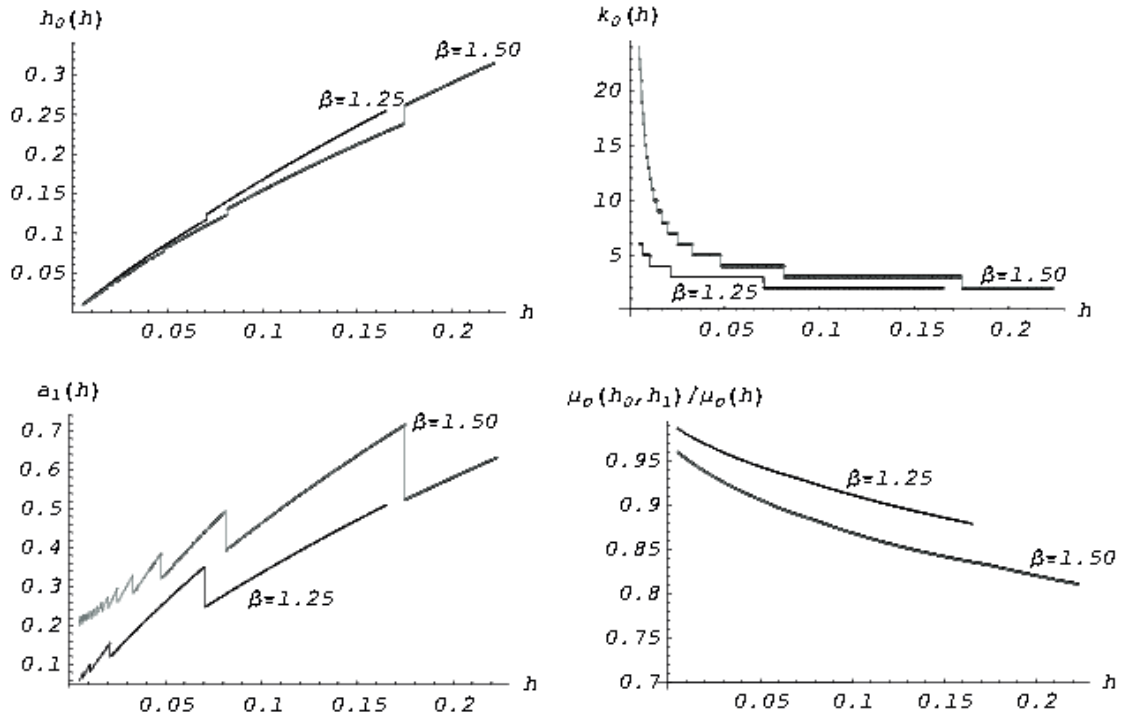


Figure 5. Comparison of FSI and VSI $\bar{X}-S^2$ chart with sample size $n=5$ under out-of-control shift in the variance from σ_{in}^2 to $\sigma_{out}^2 = k^2\sigma_{in}^2$, $k^2=2.00$.

Weibull form parameter $\beta = 1.25$ and $\beta = 1.50$.



Weibull form parameter $\beta = 1.75$ and $\beta = 2.25$

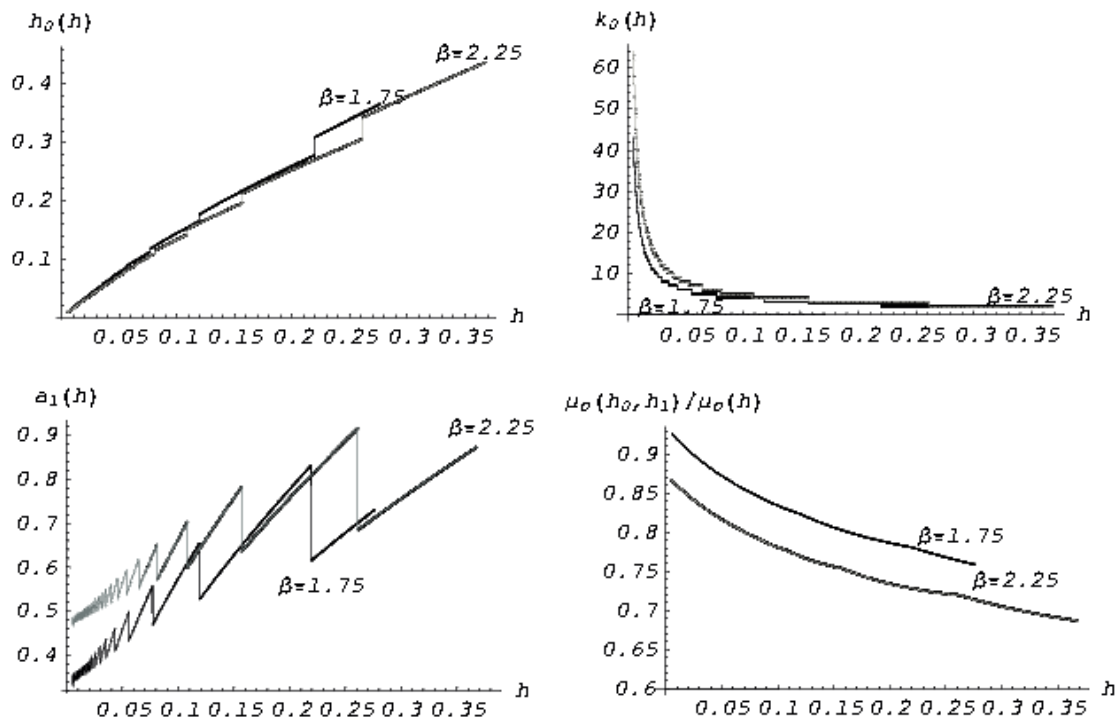


Figure 6. Comparison of FSI and VSI $\bar{X}-S^2$ chart with sample size $n=5$ under out-of-control shift in the mean from μ_{in} to $\mu_{out} = \mu_{in} + \sigma_{in}$, and in the variance from σ_{in}^2 to $\sigma_{out}^2 = 2\sigma_{in}^2$.

The range of the FSI sampling distance h is restricted to values smaller than the 10% quantile of the failure time distribution. Larger values of h are unrealistic. The lower bound for h is $h \geq 0.005$ so that all practically relevant cases will be covered. The infinite sums in the expressions for the average number of false alarms and for the expected time of out-of-control operation were approximated by finite summations. Sufficient precision was achieved by selecting the truncation points according to inequalities for the end pieces.

Each of the figures 1 through 6 consists of two parts (upper part, lower part) where each part covers two cases of the Weibull form parameter β . Each of the two parts of a figure contains four graphs. By the upper left-hand graph the VSI sampling distance $h_0 = h_0(h)$ can be determined from a given FSI sampling distance h . The upper right-hand graph shows the number of samples $k_0 = k_0(h)$ taken with distance h_0 until the switching time $a_1 = k_0 h_0$. The lower left-hand graph shows the switching time $a_1 = k_0 h_0$. After the switching time a_1 , the sampling distance is $h_1 = 0.5 h_0$. The lower right-hand graph displays the comparative performance ratios $\mu_o(h_0, h_1)/\mu_o(h)$ of the expected times of out-of-control-operation.

Figures 1 through 6 demonstrate the following properties of comparatively designed VSI charts. Throughout, the first VSI sampling distance $h_0(h)$ is considerably larger than the FSI distance h , with larger differences for small h and smaller differences for increasing h . Thus the VSI chart is a distinct alternative to the FSI chart, and a better alternative as obvious from the performance ratios $\mu_o(h_0, h_1)/\mu_o(h)$ which are considerably smaller than 1. Conforming to intuition, the comparative performance ratios $\mu_o(h_0, h_1)/\mu_o(h)$ decrease in h . For small h , the advantage of the VSI chart over the FSI chart is smaller. For all values of the Weibull form parameter β , $k_0(h)$ decreases very rapidly for small values of h , approximately for $h \leq 0.05$. For larger values of h , $k_0(h)$ varies very slowly, adopting values $4 \leq k_0(h) \leq 8$.

For fixed FSI distance h , the ratios $\mu_o(h_0, h_1)/\mu_o(h)$ are decreasing in the Weibull form parameter β : The more rigorous the aging pattern of the process, the better the performance of the VSI chart.

8. Numerical Example

To illustrate the use of figures 1 through 6 we consider a simple numerical example. Let the process quality parameter be the mean μ of some normally distributed quality characteristic. Let the process time be measured in hours of operation. A process failure shifts the mean by one unit $1.00 \cdot \sigma$ of the standard deviation from the in-control target value μ_{in} to the out-of control value $\mu_{out} = \mu_{in} + \sigma$. From historic process documentation of the time to failure D , let a Weibull distribution be estimated with values $\beta = 1.25$ of the form parameter and $\vartheta = 51.00$ of the scale parameter. The mean time to failure is $\mu_D = 47.50$, i.e., on the average a process failure (shift) occurs after 47.50 hours of operation. The standard deviation of the time to failure is $\sigma_D = 38.24$. In view of the large standard deviation the process is monitored by a Shewhart \bar{X} chart with three-sigma limits and with sample size $n = 5$.

Under the periodic FSI policy, samples are taken every two hours, i.e., the FSI sampling distance is $h = 2.00$. Following the design rule 1, the corresponding VSI bipartition chart can be determined from the upper part of figure 1 by applying formula (18). We find $h_{0,\vartheta}(h) = \vartheta h_{0,1}(h/\vartheta) \approx 51.00 h_{0,1}(0.04) \approx 51.00 \cdot 0.07 \approx 3.60$, $k_{0,\vartheta}(h) = k_{0,1}(h/\vartheta) \approx 5$. Under the VSI chart, the first 5 samples should be taken at distances of approximately three and a half hours, the remaining samples at distances of approximately one hour and

45 minutes. The lower right-hand graph of the upper part of figure 1 shows that the VSI chart yields a reduction in average out-of-control operation time of approximately 8%.

9. Conclusion

1) We have developed a novel framework for VSI policies depending on the distribution of the time to failure in the process. This framework represents a reasonable attempt to formally address Wheeler's ([21], p. 142) statement that the rate at which the process can change should determine the rationale of the sampling frequency.

2) Section 5 suggests a simple policy for VSI charts, comparatively determined from a prescribed FSI chart: the bipartition policy with one switching time, based on the rules 1 and 2, and on experience gained on shop floor. This is a quite straightforward design principle with the potential to be considered a basic tool. Indeed, this design approach is a general strategy to promote VSI charts as the more economical alternative to well-established FSI charts.

3) We have developed a framework for the design of VSI Shewhart charts – two sided Shewhart \bar{X} chart and the combined $\bar{X}-S^2$ charts under the three shift models SM1, SM2 and SM3, respectively – under a scale family of failure time distributions, as defined in Section 6. When the time to failure is Weibull, the comparative design of a VSI bipartition chart is easily determined by graphs of the type presented in Section 7, for any value of the scale parameter. Other lifetime distributions of the scale family for which designing is likewise straightforward are the Gamma and the Birnbaum-Saunders. These graphs show that a VSI chart with the same average amount of sampling as a given FSI considerably reduces the average time of out-of-control operation. Moreover, the VSI bipartition chart presented is in line with the practitioners' concept of sampling more frequently as a tool or machine approaches the end of an operation cycle. The numerical example presented in section 8 shows how easy it is to use the graphs. For calculations under further values of the relevant parameters (sample size n , shift size, Weibull parameters) graphs and software are made available to the interested reader on the website <http://statistik.mathematik.uni-wuerzburg.de/projekte/shewartcharts>.

4) For future research, the following issues are important: i) examine further and more general classes of failure time distributions, but bearing in mind that handy graphs can be built only if the adjustable parameter (the β in this article) is one dimensional; ii) extend the comparative design approach to VSSI charts with both sampling distance and sample size variable as considered by Costa [4]; iii) consider other types of control charts such as CUSUM or EWMA, provided the alarm probabilities can be derived adequately; iv) assume more complex process models, in particular involving autocorrelation; v) study policies with increased frequency of reducing the sampling distance, e.g., more than one bipartition.

5) Model generalization as stipulated under 4), above, is not the only issue to make the framework useful for industry. It is also very important to communicate the scheme to industry. The authors declare their interest and availability for the dialogue with interested practitioners to discuss problems of shop floor implementation and to clarify matters of theory or notation used. Unlike the case treated here, the inevitably more complex theory and notation of studies in VSI schemes, in comparison with the traditional FSI schemes, seriously obstructs industrial implementation, see [2].

Acknowledgments

This paper is supported by funding from the “Growth” program of the European Community and was prepared in collaboration by member organizations of the Thematic Network-Pro-ENBIS-EC contract number G6RT-CT-2001-05059.

References

1. Amin, R. W. and Miller, R. W. (1993). A Robustness Study of \bar{X} Charts with Variable Sampling Intervals. *Journal of Quality Technology*, 25, 35-44.
2. Baxley, R. V. (1995). An Application of Variable Sampling Interval Control Charts. *Journal of Quality Technology*, 27, 275-282.
3. von Collani, E. (1990). Wirtschaftliche Qualitätskontrolle – eine Übersicht über einige neue Ergebnisse. *OR Spektrum*, 12, 1-23.
4. Costa, A. F. B. (1997). \bar{X} Chart with Variable Sample Size and Sampling Intervals. *Journal of Quality Technology*, 29, 197-204.
5. Duncan, A. J. (1956). The Economic Design of \bar{X} -Charts Used to Maintain Current Control of a Process. *Journal of the American Statistical Association*, 51, 228-242.
6. Ho, C. and Case, K. E. (1994). Economic Design of Control Charts: A Literature Review for 1981-1991. *Journal of Quality Technology*, 26, 39-53.
7. Johnson, N. L., Kotz, S., Balakrishnan, N. (1994). *Continuous Univariate Distributions*, Volume 1, Second Edition. John Wiley & Sons, New York.
8. Montgomery, D. C. (1980). The Economic Design of Control Charts: A Review and Literature Survey. *Journal of Quality Technology*, 12, 75-87.
9. Park, C., and Reynolds, M. R. (1999). Economic Design of a Variable Sampling Rate \bar{X} -Chart. *Journal of Quality Technology*, 31, 427-443.
10. Ramalhoto, M. F. and Morais, M. (1999). Shewhart Control Charts for the Scale Parameter of a Weibull Control Variable with Fixed and Variable Sampling Intervals. *Journal of Applied Statistics*, 26, 129-160.
11. Ramalhoto, M. F., Göb, R., Pievatolo, A., and Evandt, O. (2004). Statistical Process Control Procedures in Relation with Reliability Engineering. In *Probabilistic Safety Assessment and Management PSAM7/ESREL04* (Edited by C. Spitzer, U.Schmocker, V. N. Dang), 3048-3059. Springer, London.
12. Reynolds, M. R. (1986). Optimal Two-Sided Variable Sampling Interval Control Charts for the Exponential Family. *Technical Report 86-4*, Virginia Polytechnic Institute and State University, Department of Statistics.
13. Reynolds, M. R. (1989). Optimal Variable Sampling Interval Control Charts. *Sequential Analysis*, 8(4), 361-379.
14. Reynolds, M. R. and Arnold, J. C. (1989). Optimal One-Sided Shewhart Control Charts with Variable Sampling Intervals. *Sequential Analysis* 8(1), 51-77.
15. Reynolds, M. R., Amin, R. W., Arnold, J. C., and Nachlas, J.A. (1988). \bar{X} Charts with Variable Sampling Intervals. *Technometrics*, 30(2), 181-192.
16. Reynolds, M. R., Arnold, J. C., and Baik, J. W. (1996). Variable Sampling Interval \bar{X} Charts in the Presence of Correlation. *Journal of Quality Technology*, 28, 1-28.
17. Runger, G. C., and Pignatiello, J. J. Jr. (1991). Adaptive Sampling for Process Control. *Journal of Quality Technology*, 23, 135-155.
18. Runger, G. C., and Montgomery, D. C. (1993). Adaptive Sampling Enhancements for

Shewhart Control Charts. *IIE Transactions*, 25, 41-51.

19. Ryan, T. (2000). *Statistical Methods For Quality Improvement*, Second Edition. John Wiley & Sons, New York.
20. Shewhart, W. A. (1931). *Economic Control of Quality of Manufactured Product*. D. van Nostrand Company, Princeton, New Jersey.
21. Wheeler, D. J. (1995). *Advanced Topics in Statistical Process Control*. SPC Press, Knoxville, Tennessee.

Appendix

A. A Summation Formula

The following summation formula is used in appendices B and C.

Proposition. Let L be a univariate discrete random variable which adopts the values $0 = x_0 < x_1 < x_2 < \dots$. Then we have

$$\sum_{i=1}^{\infty} x_i P(L = x_i) = \sum_{i=1}^{\infty} (x_i - x_{i-1}) P(L \geq x_i). \tag{22}$$

The proof proceeds either directly or by considering the formula as a special instance of the formula for integration by parts.

B. Calculation of the Average Cycle Length

The cycle can terminate only at one of the sampling times $t_1 < t_2 < t_3 < \dots$. We calculate the conditional distribution of the cycle length Z under the condition that the disturbance time D adopts values in the time intervals $I_{m,i}$, which for $m=0, \dots, s$ are defined by

$$I_{m,i} = (a_m + ih_m; a_m + (i+1)h_m] \quad \text{for } i=0, \dots, k_m - 1. \tag{23}$$

From equation (23) it is clear that the family $I_{m,i}$, $m=0, \dots, s$, $i=0, \dots, k_m - 1$ is a disjoint partition of the half axis $(0; +\infty)$. The natural succession of the intervals is

$$I_{0,0}, \dots, I_{0,k_0-1}, I_{1,0}, \dots, I_{1,k_1-1}, \dots, I_{s-1,0}, \dots, I_{s-1,k_{s-1}-1}, I_{s,0}, I_{s,1}, \dots$$

For $m, l=0, \dots, s$, $i=0, \dots, k_m - 1$, $j=1, \dots, k_l$, we obtain the conditional probabilities

$$P(Z = a_l + jh_l | D \in I_{m,i}) = \begin{cases} (1 - p_{\text{out}})^{j-i-1} p_{\text{out}}, & \text{if } l = m, j \geq i + 1, \\ (1 - p_{\text{out}})^{k_m + \dots + k_{l-1} + j - i - 1} p_{\text{out}}, & \text{if } l > m, \\ 0, & \text{otherwise.} \end{cases} \tag{24}$$

and

$$P(Z \geq a_l + jh_l | D \in I_{m,i}) = \begin{cases} (1 - p_{\text{out}})^{j-i-1}, & \text{if } l = m, j \geq i + 1, \\ (1 - p_{\text{out}})^{k_m + \dots + k_{l-1} + j - i - 1}, & \text{if } l > m, \\ 0, & \text{otherwise.} \end{cases} \tag{25}$$

By equation (22) we obtain the conditional expectation

$$e_{m,i} = E[Z | D \in I_{m,i}] = \sum_{l,j} (a_l + jh_l) P(Z = a_l + jh_l | D \in I_{m,i})$$

$$\begin{aligned}
 &= (a_m + (i+1)h_m)P(Z \geq a_m + (i+1)h_m | D \in I_{m,i}) + \\
 &\quad h_m \sum_{j=i+2}^{k_m} P(Z \geq a_m + jh_m | D \in I_{m,i}) + \\
 &\quad h_{m+1} \sum_{j=1}^{k_{m+1}} P(Z \geq a_{m+1} + jh_{m+1} | D \in I_{m,i}) + \dots + \\
 &\quad h_{s-1} \sum_{j=1}^{k_{s-1}} P(Z \geq a_{s-1} + jh_{s-1} | D \in I_{m,i}) + h_s \sum_{j=1}^{\infty} P(Z \geq a_s + jh_s | D \in I_{m,i}) \\
 &= (a_m + (i+1)h_m) + h_m(1 - p_{\text{out}}) \frac{1 - (1 - p_{\text{out}})^{k_m - i - 1}}{p_{\text{out}}} + \\
 &\quad h_{m+1}(1 - p_{\text{out}})^{k_m - i} \frac{1 - (1 - p_{\text{out}})^{k_{m+1}}}{p_{\text{out}}} + \dots + \\
 &\quad h_{s-1}(1 - p_{\text{out}})^{k_m + \dots + k_{s-2} - i} \frac{1 - (1 - p_{\text{out}})^{k_{s-1}}}{p_{\text{out}}} + h_s(1 - p_{\text{out}})^{k_m + \dots + k_{s-1} - i} \frac{1}{p_{\text{out}}} \\
 &= a_m + ih_m + \frac{h_m}{p_{\text{out}}} + (h_{m+1} - h_m) \frac{(1 - p_{\text{out}})^{k_m - i}}{p_{\text{out}}} + \\
 &\quad (h_{m+2} - h_{m+1}) \frac{(1 - p_{\text{out}})^{k_m + k_{m+1} - i}}{p_{\text{out}}} + \dots + (h_s - h_{s-1}) \frac{(1 - p_{\text{out}})^{k_m + \dots + k_{s-1} - i}}{p_{\text{out}}} \tag{26}
 \end{aligned}$$

For $m = 0, \dots, s$, $i = 0, \dots, k_m - 1$, let $\Delta_{m,i}$ be defined by equation (6). From the definition of a_i by equation (3) and from equation (26) we obtain for $m = 0, \dots, s$, $i = 0, \dots, k_m - 1$

$$\Delta_{m,i} = \begin{cases} e_{m,i} - e_{m,i-1} & , \text{ if } 1 \leq i \leq k_m - 1 \\ e_{m,0} - e_{m-1, k_{m-1} - 1} & , \text{ if } i = 0 \end{cases} \tag{27}$$

where we let $e_{-1, k_{-1} - 1} = 0$ by definition. The unconditional expected cycle length is obtained by averaging over the conditional expectations $e_{m,i}$ with weights $P(D \in I_{m,i})$:

$$\mu_Z = E[Z] = \sum_{m=0}^s \sum_{i=0}^{k_m - 1} e_{m,i} P(D \in I_{m,i}). \tag{28}$$

By equation (22) we obtain equation (5).

C. Calculation of the Average Number of False Alarms.

Let the time intervals $I_{m,i}$ be defined by equation (23). The conditional distribution of the number A_{false} of false alarms under the condition $D \in I_{m,i}$ follows a binomial distribution with parameters $k_0 + \dots + k_{m-1} + i$ (number of independent trials, i.e., number of samples inspected) and p_{in} (probability of success in one trial, i.e., the probability of a false alarm). Hence the conditional expected number of false alarms is

$$E[A_{\text{false}} | D \in I_{m,i}] = (k_0 + \dots + k_{m-1} + i) p_{\text{in}} \tag{29}$$

for $m = 0, \dots, s$, $i = 0, \dots, k_m - 1$. Averaging over the conditional expectations and applying equation (22) we obtain the unconditional expectation as given by equation (8).

Authors' Biographies:

Rainer Göb received his doctoral degrees from the University of Würzburg, Germany, in 1992 and 1996. He has been teaching as a professor of statistics at the University of Würzburg since 1996. His research interest is industrial statistics, in particular, statistical quality control, statistics in manufacturing and business management. He is working as an industrial consultant as the head of the Methodica Consulting group.

M. F. Ramalhoto is a Ph.D. from University College of London, and is a Professor of Applied Probability and Statistics at the Technical University of Lisbon-IST. Her research interests are in the areas of applied stochastic processes, queueing theory, data analysis, stochastics for reliability, and quality improvement and innovation, and has several papers published in statistics, operations research, and applied stochastic processes international journals. She is a member of ISI, founder member and former vice-president of ENBIS, and is an expert for the European Commission Fifth and Sixth Frameworks. She has been a visiting scientist in several universities, namely, Berkeley, MIT, and Princeton.

Antonio Pievatolo received his M.S. degree and the Doctorate in Statistics from the University of Padua, Italy, in 1992 and 1998, respectively. He has been a research scientist at CNR-IMATI (National Research Council of Italy, Institute of Applied Mathematics and Computer Science) since 1997. His research interests include general statistical modelling, point processes, and reliability.